

Electronic Supplementary Information (ESI)

Semi-hydrogenation of α,β -unsaturated aldehydes over sandwich-structured nanocatalysts prepared by phase-transformation of thin-film Al_2O_3 to Al-TCPP

Bin Chen,^{a,b} Xin Yang,^{a,} Yinan Xu,^c Siyuan Hu,^a Xiaoli Zeng,^a Yiping Liu,^a Kok Bing Tan,^b Jiale Huang,^{b,*} and Guowu Zhan^{a,*}*

^a College of Chemical Engineering, Integrated Nanocatalysts Institute (INCI), Huaqiao University, 668 Jimei Blvd., Xiamen, Fujian, 361021, P. R. China

^b Department of Chemical and Biochemical Engineering, College of Chemistry and Chemical Engineering, Xiamen University, 422 Siming South Road, Xiamen, Fujian 361005, P. R. China

^c Davidson School of Chemical Engineering, Purdue University, 480 Stadium Mall Drive, West Lafayette, IN 47907, USA

**Corresponding Authors E-mail: gwzhan@hqu.edu.cn (G. Zhan), yangxin@hqu.edu.cn (X. Yang), and cola@xmu.edu.cn (J. Huang)*

Table of Contents

Supporting Tables

Table S1. ICP analysis results of different catalyst samples.	4
Table S2. Textural properties of different catalyst samples.	5
Table S3. The comparisons of different catalyst performances for selective hydrogenation of CAL.	6
Table S4. The amount of CO molecules adsorbed on the catalysts measured by CO pulsed adsorption.	8

Supporting Scheme

Scheme S1. (a) The traditional synthetic route of MOFs@MNPs@MOFs materials, and (b) the novel synthetic strategy of MOFs@MNPs@MOFs proposed in this work.	9
---	---

Supporting Figures

Figure S1. (a) TEM image at low magnification of MIL-88B(Fe)@Pt@Al-TCPP catalyst. (b) Particle size distribution histogram of Pt NPs on MIL-88B(Fe)@Pt@Al-TCPP.	10
Figure S2. Powder XRD pattern of the pure Al-TCPP.	11
Figure S3. Solid-state UV-vis spectra of MIL-88B(Fe)@Pt@Al ₂ O ₃ and MIL-88B(Fe)@Pt@Al-TCPP samples.	12
Figure S4. TGA curve of MIL-88B(Fe) under air atmosphere.	13
Figure S5. Molecular structure of cinnamaldehyde (CAL, 1.05 × 0.65 nm). Color code: carbon-gray, oxygen-red, and hydrogen-blue.	14
Figure S6. FTIR spectra of different samples: CAL molecule, MIL-88B(Fe), and MIL-88B(Fe)/CAL mixture.	15
Figure S7. FTIR spectra of different samples: CAL molecule, Al-TCPP, and Al-TCPP/CAL mixture.	16
Figure S8. Digital photos show contact angles of a water droplet on different substrates such as (a) MIL-88B(Fe) and (b) MIL-88B(Fe)@Pt@Al ₂ O ₃ catalysts. The catalytic conversion and selectivity of MIL-88B(Fe)@Pt and MIL-88B(Fe)@Pt@Al ₂ O ₃ catalysts for selective hydrogenation of CAL.	17
Figure S9. FTIR spectra of pure CAL molecule, MIL-88B(Fe)@Pt@Al-TCPP, and CAL adsorbed on MIL-88B(Fe)@Pt@Al-TCPP.	18
Figure S10. FTIR spectra of MIL-88B(Fe)@Pt@Al-TCPP produced by using ALD Al ₂ O ₃ with different layer thicknesses.	19
Figure S11. (a-d) Representative SEM images of MIL-88B(Fe)@Pt@Al-TCPP catalysts produced by using ALD Al ₂ O ₃ with different layer thicknesses.	20

Figure S12. XRD patterns of MIL-88B(Fe)@Pt@Al-TCPP produced by using ALD Al ₂ O ₃ with different layer thicknesses.	21
Figure S13. (a-b) The conversion and selectivity data during the recycling experiments using MIL-88B(Fe)@Pt@Al-TCPP catalyst. (c-d) XRD pattern and SEM image of MIL-88B(Fe)@Pt@Al-TCPP catalyst after 5 cycles.	22
Figure S14. (a) N ₂ physisorption isotherms at 77 K and (b) pore-size distribution curve of MIL-88B(Fe)@Pt@Al-TCPP after 5 cycles.	23
Figure S15. The conversion and selectivity data of furfural (FA) selective hydrogenation using MIL-88B(Fe)@Pt@Al-TCPP catalyst.	24
Figure S16. High-resolution O 1s spectra of MIL-88B(Fe), MIL-88B(Fe)@Pt, MIL-88B(Fe)@Pt@Al ₂ O ₃ , and MIL-88B(Fe)@Pt@Al-TCPP catalysts.	25
Figure S17. The bond length of the C=O double bond of (a) the free CAL molecule. The bond length of the C=O double bond of the CAL molecule adsorbed on (b) Pt NPs, (c) MIL-88B(Fe), and (d) Al-TCPP.	26
Figure S18. The bond angle of the C=O double bond of (a) the free CAL molecule. The bond angle of the C=O double bond of the CAL molecule adsorbed on (b) Pt NPs, (c) MIL-88B(Fe), and (d) Al-TCPP.	27

Table S1. ICP analysis results of different catalyst samples.

Catalyst	Fe/wt%	Pt/wt%	Al/wt%
MIL-88B(Fe)@Pt	15.4	3.3	nil
MIL-88B(Fe)@Pt@Al ₂ O ₃	12	2.9	12.4
MIL-88B(Fe)@Pt@Al-TCPP	8.2	1.7	8.5

Table S2. Textural properties of different catalyst samples.

Sample	S_{BET} ($\text{m}^2 \text{g}^{-1}$)	S_{meso} ($\text{m}^2 \text{g}^{-1}$)	V_{t} ($\text{cm}^3 \text{g}^{-1}$)	V_{meso} ($\text{cm}^3 \text{g}^{-1}$)
MIL-88B(Fe)	100.3	100.3	1.41	0
MIL-88B(Fe)@Pt	45.4	45.3	0.25	0
MIL-88B(Fe)@Pt@Al ₂ O ₃	42.2	42.2	0.35	0
MIL-88B(Fe)@Pt@Al-TCPP	472.2	243.2	1.30	0.097

Notes: S_{BET} is the BET-specific surface area, S_{meso} is the specific mesopore surface area estimated by subtracting S_{micro} , the t-plot-specific micropore surface area calculated from the N₂ adsorption-desorption isotherm from S_{BET} . V_{t} is the total specific pore volume determined by using the adsorption branch of the N₂ isotherm at $P/P_0=0.99$, and V_{meso} is the specific mesopore volume obtained from the BJH cumulative specific desorption volume.

Table S3. The comparisons of different catalyst performances for selective hydrogenation of CAL.

Catalysts	Temperature (°C)	P _{H2} (bar)	Time (min)	Pt loading (%)	Conversion (%)	COL selectivity (%)	TOF _{Pt} (h ⁻¹)	References
Pt/SiO ₂	150	10	15	5.0	14.0	13.0	468	[1]
Pt _{0.1} Au/SiO ₂	150	10	15	10.0	16.0	21.0	11196	[2]
Pt/SBA-15	90	20	60	6.5	22.3	40.9	756	[3]
Pt/Al ₂ O ₃ @SBA-15	90	20	60	5.3	34.9	64.7	972	[3]
Pt/TiH ₂	100	40	30	1.0	30.0	88.7	399	[4]
PtCo/CNTs	60	25	90	0.5	92.4	93.6	500	[5]
Pt/MgAl-LDH	60	10	120	2.0	79.7	85.4	318	[6]
Pt@UiO-66-NH ₂	25	40	2640	1.0	85.9	87.9	23	[7]
MIL-101@Pt@FeP-CMP ^a	25	30	15	n.a.	97.9	82.7	1464	[8]
MIL-101(Fe)@Pt@MIL-101(Fe)	25	30	1440	4.7	94.3	97	13	[9]
Pt/Fe-LDH	110	10	120	2.8	90.0	92.0	17.4	[10]
Pt/Fe ₃ O ₄	30	50	150	2.5	94.2	92.2	6	[11]

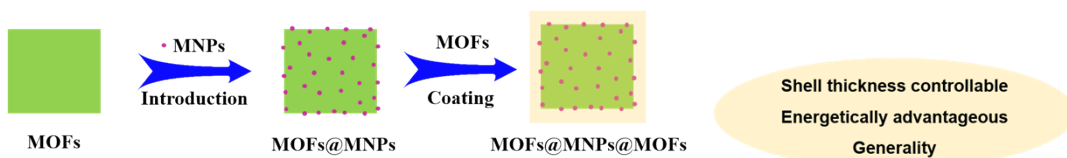
Pt ₃₀ Fe ₃₀ /Al ₂ O ₃	60	20	480	0.4	75.0%	84.0%	n.a.	[12]
Fe _{0.33} Pt _{0.67} -C10F ^b	50	1	60	0.62	71.1%	94%	n.a.	[13]
Pt-FeO _x /MoO _{3-y}	30	10	180	3.7	68.8%	91.3%	n.a.	[14]
MIL-88B (Fe)@Pt@Al-TCPP	60	30	240	1.7	95.0	85.0	48	this work
MIL-88B (Fe)@Pt@Al ₂ O ₃	60	30	240	2.9	61.0	64.0	11	this work
MIL-88B (Fe)@Pt	60	30	240	3.3	35.0	64.0	5.5	this work

Notes: ^aFeP-CMPs is a conjugated micro- and mesoporous polymers with iron(III) porphyrin. ^bC10F is an F-containing carboxylate surface ligand with a carbon chain length of 10.

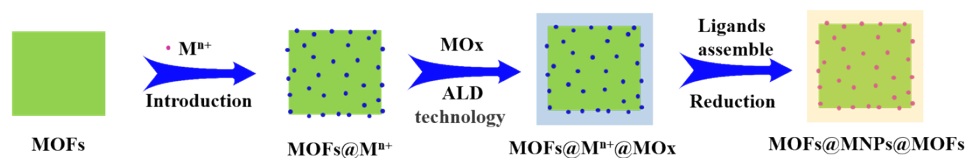
Table S4. The amount of CO molecules adsorbed on the catalysts measured by CO pulsed adsorption.

Sample	CO adsorption quantity ($\mu\text{mol/g}$)	Pt dispersion
MIL-88B(Fe)	838.5	-
MIL-88B(Fe)@Pt	883.6	0.266
MIL-88B(Fe)@Al ₂ O ₃	1473.0	-
MIL-88B(Fe)@Pt@Al ₂ O ₃	1601.3	0.8655
MIL-88B(Fe)@Al-TCPP	1573.0	-
MIL-88B(Fe)@Pt@Al-TCPP	1960.0	>0.95

a Traditional Synthesis Methods of MOFs@MNPs@MOFs



b New strategies for the synthesis of MOFs@MNPs@MOFs



Scheme S1. (a) The traditional synthetic route of MOFs@MNPs@MOFs materials, and (b) the novel synthetic strategy of MOFs@MNPs@MOFs proposed in this work.

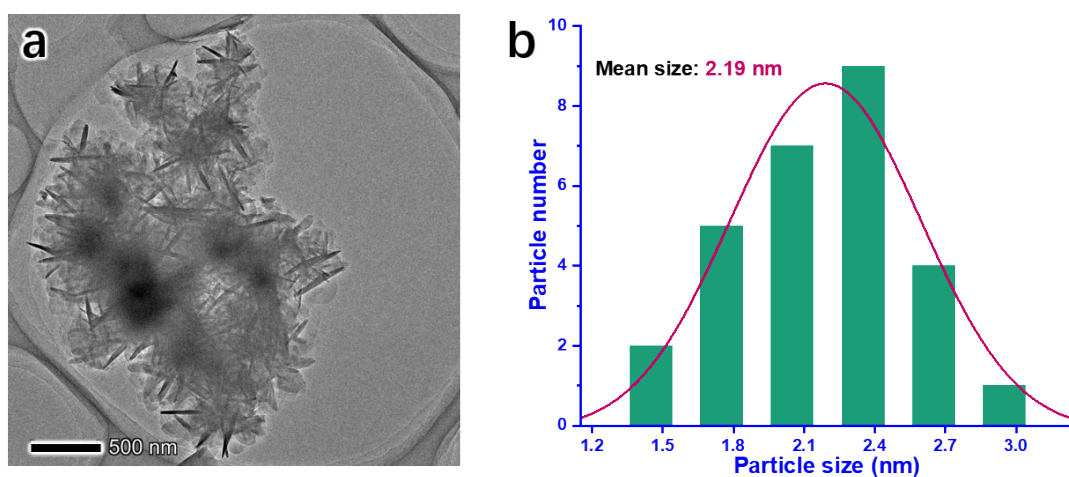


Figure S1. (a) TEM image at low magnification of MIL-88B(Fe)@Pt@Al-TCPP catalyst. (b) Particle size distribution histogram of Pt NPs on MIL-88B(Fe)@Pt@Al-TCPP.

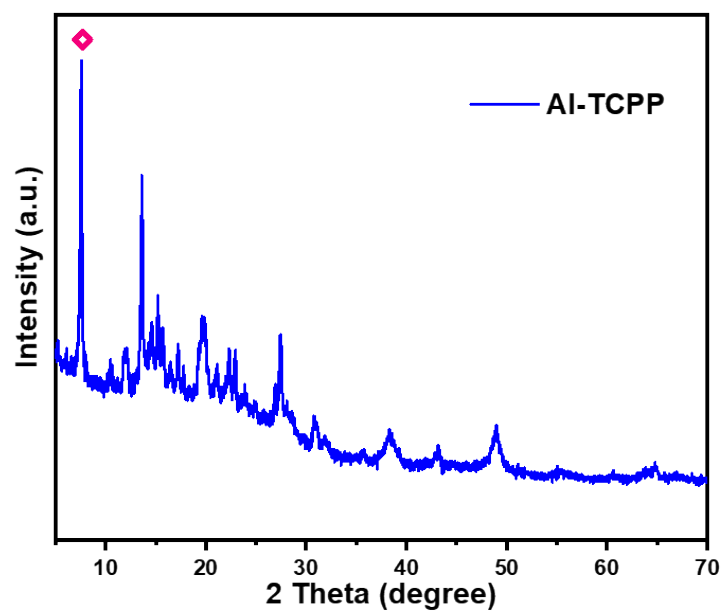


Figure S2. Powder XRD pattern of the pure Al-TCPP.

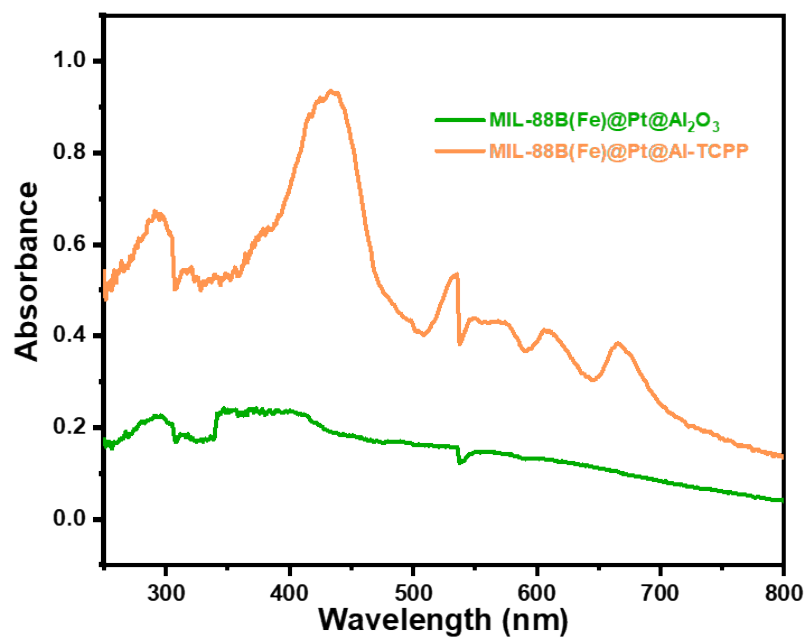


Figure S3. Solid-state UV-vis spectra of MIL-88B(Fe)@Pt@Al₂O₃ and MIL-88B(Fe)@Pt@Al-TCPP samples.

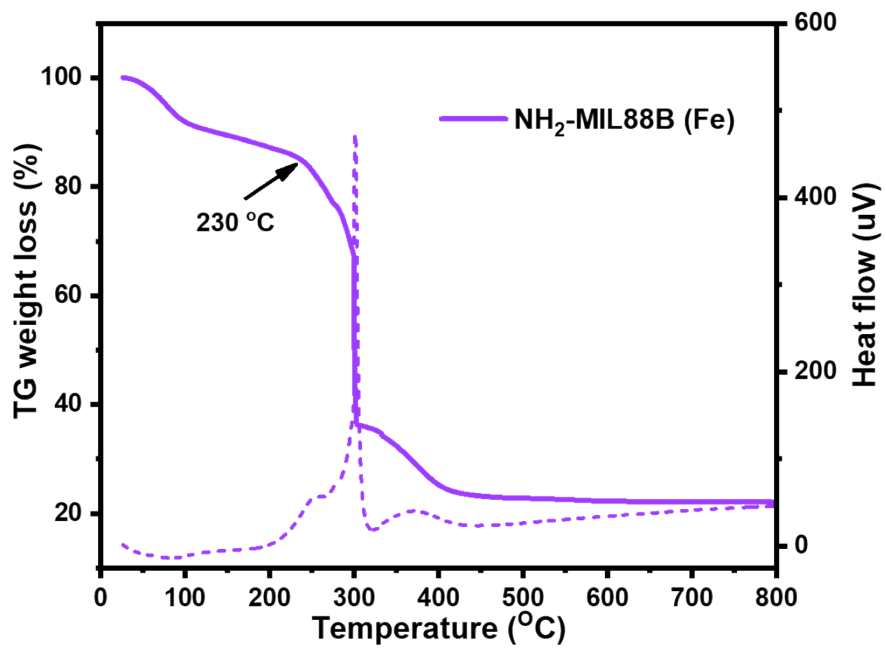


Figure S4. TGA curve of MIL-88B(Fe) under air atmosphere.

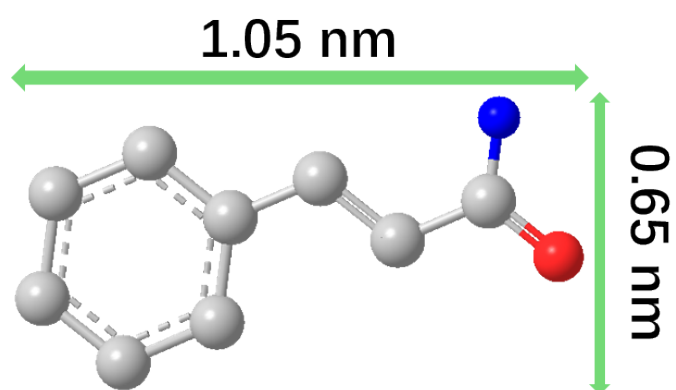


Figure S5. Molecular structure of cinnamaldehyde (CAL, 1.05×0.65 nm). Color code: carbon-gray, oxygen-red, and hydrogen-blue.

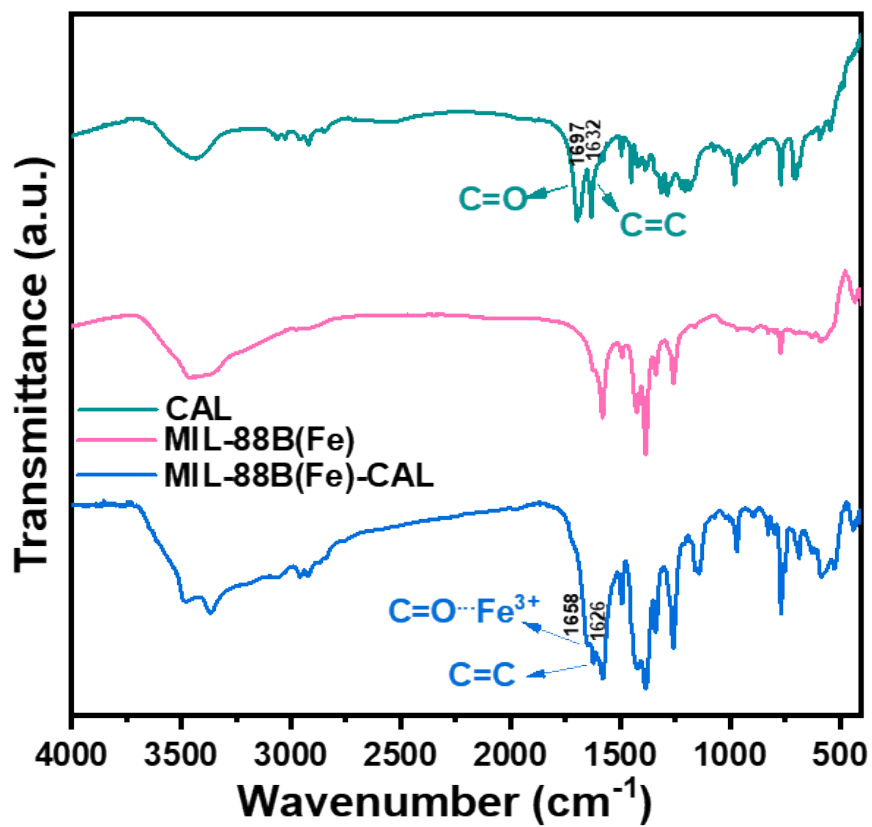


Figure S6. FTIR spectra of different samples: CAL molecule, MIL-88B(Fe), and MIL-88B(Fe)/CAL mixture.

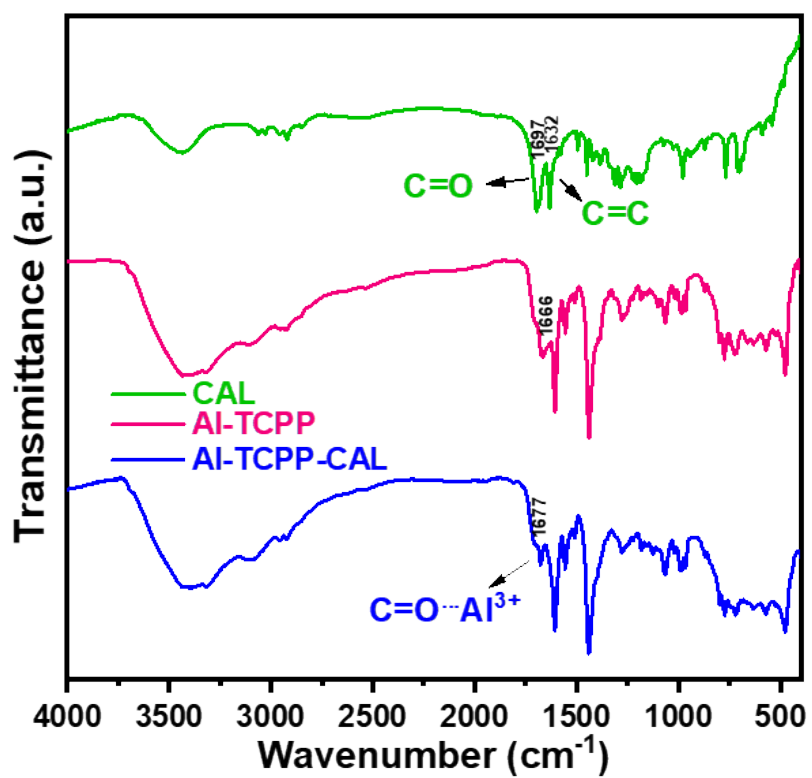


Figure S7. FTIR spectra of different samples: CAL molecule, Al-TCPP, and Al-TCPP/CAL mixture.

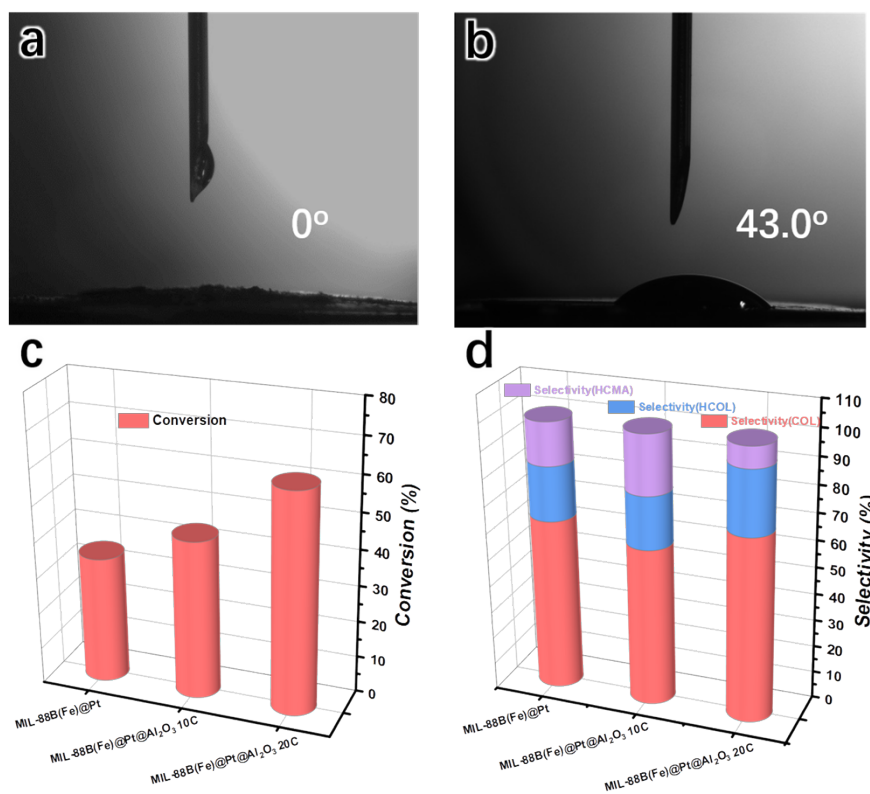


Figure S8. Digital photos show contact angles of a water droplet on different substrates such as (a) MIL-88B(Fe) and (b) MIL-88B(Fe)@Pt@Al₂O₃ catalysts. The catalytic conversion and selectivity of MIL-88B(Fe)@Pt and MIL-88B(Fe)@Pt@Al₂O₃ catalysts for selective hydrogenation of CAL.

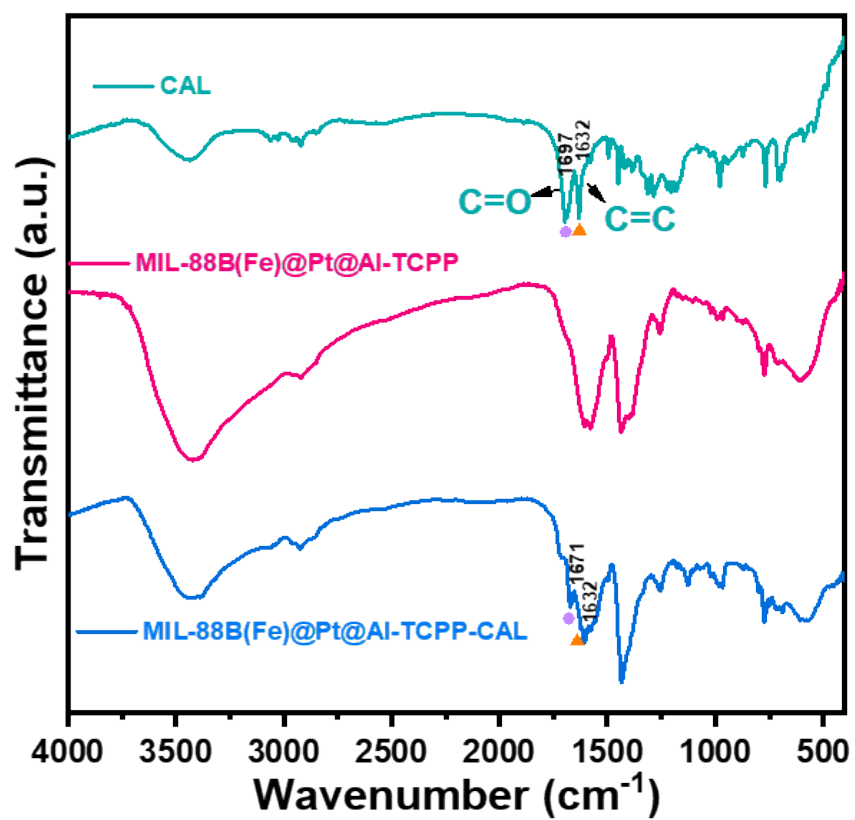


Figure S9. FTIR spectra of pure CAL molecule, MIL-88B(Fe)@Pt@Al-TCPP, and CAL adsorbed on MIL-88B(Fe)@Pt@Al-TCPP.

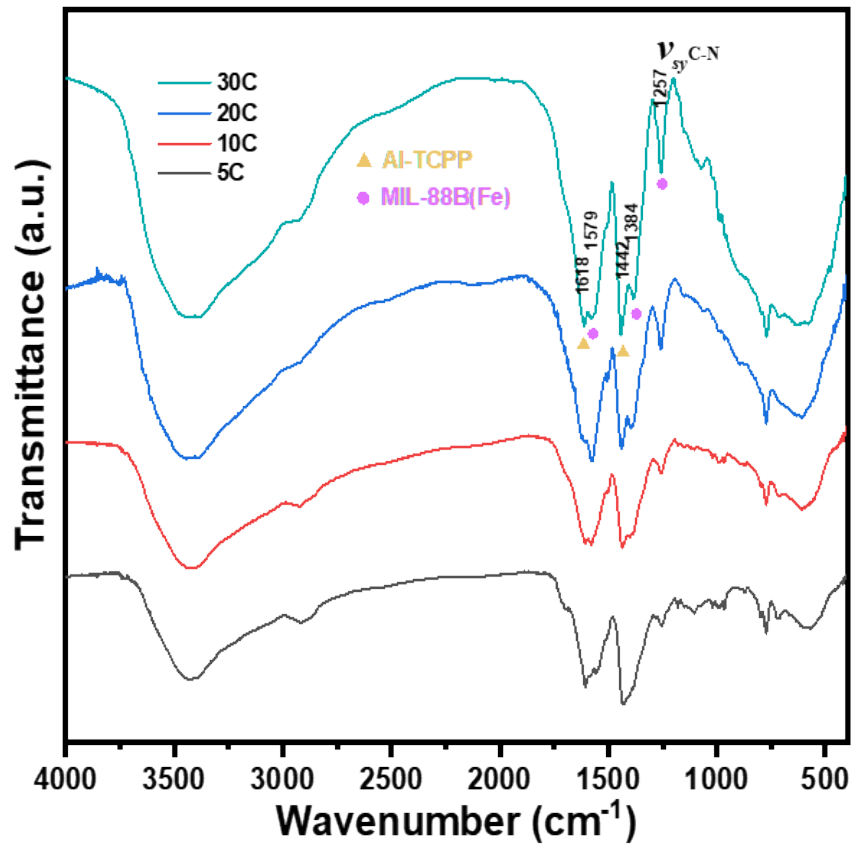


Figure S10. FTIR spectra of MIL-88B(Fe)@Pt@Al-TCPP produced by using ALD Al₂O₃ with different layer thicknesses.

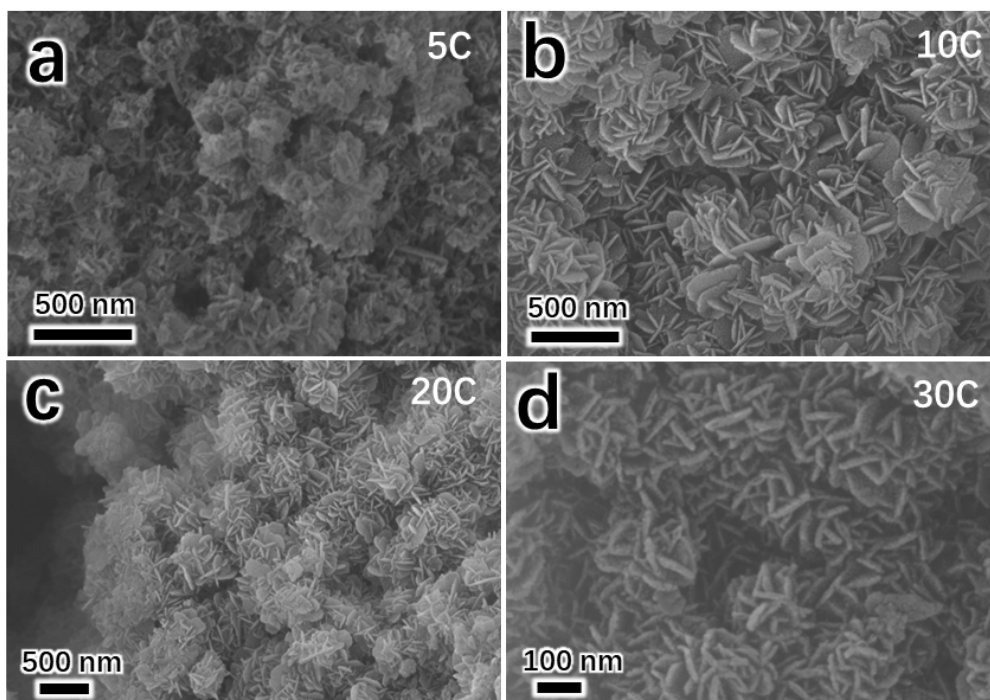


Figure S11. (a-d) Representative SEM images of MIL-88B(Fe)@Pt@Al-TCPP catalysts produced by using ALD Al₂O₃ with different layer thicknesses.

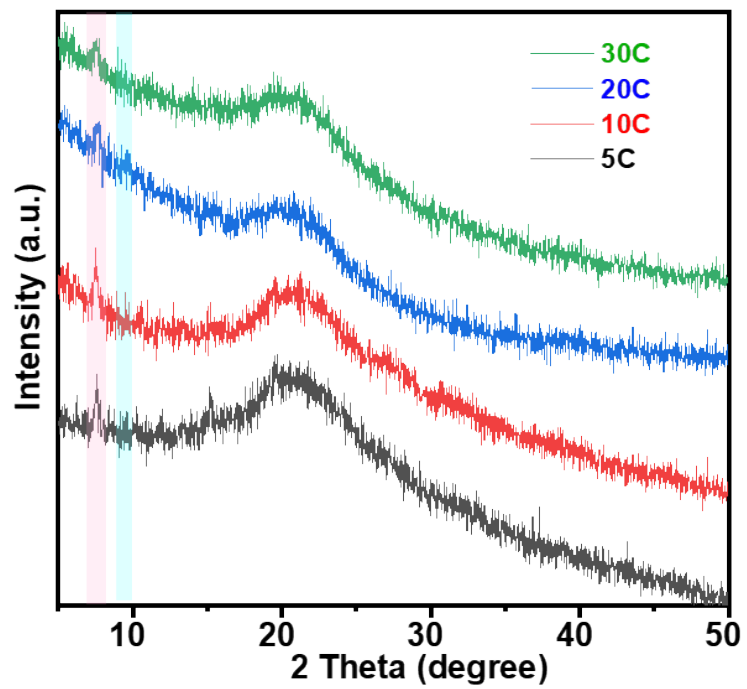


Figure S12. XRD patterns of MIL-88B(Fe)@Pt@Al-TCPP produced by using ALD Al₂O₃ with different layer thicknesses.

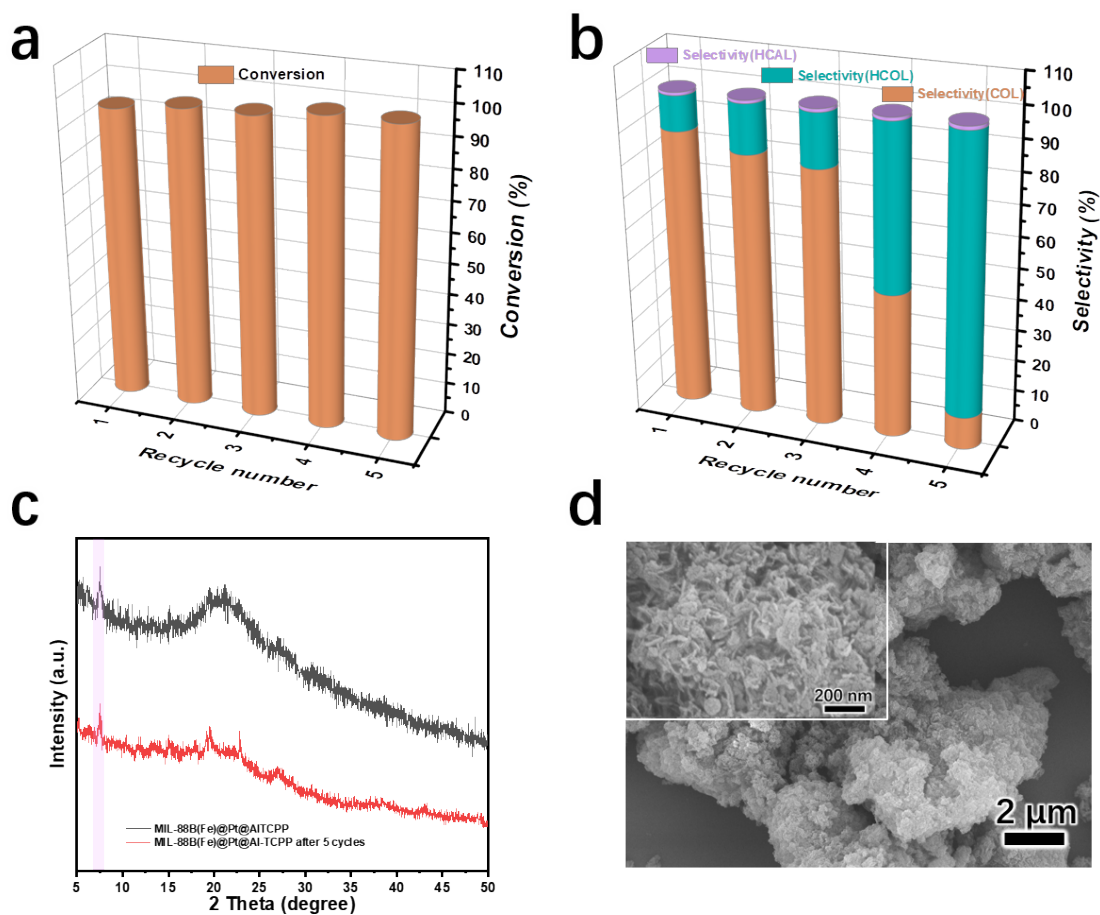


Figure S13. (a-b) The conversion and selectivity data during the recycling experiments using MIL-88B(Fe)@Pt@Al-TCPP catalyst. (c-d) XRD pattern and SEM image of MIL-88B(Fe)@Pt@Al-TCPP catalyst after 5 cycles.

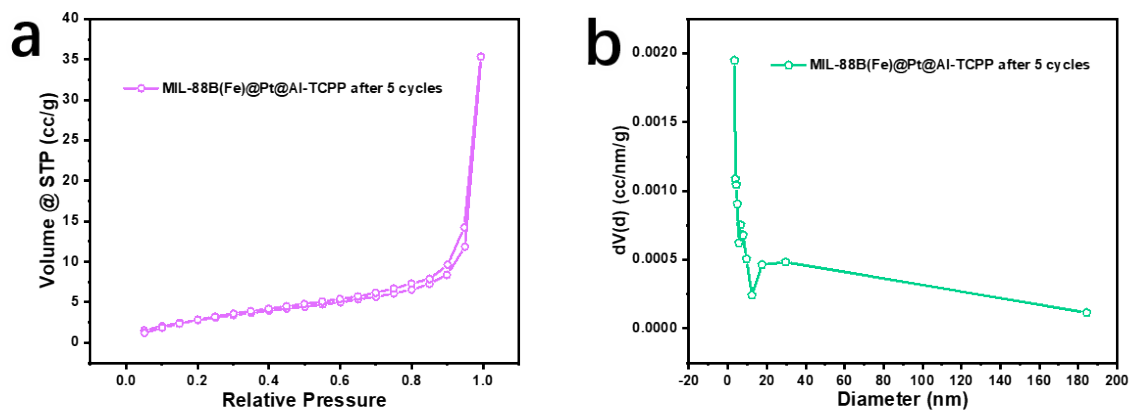


Figure S14. (a) N₂ physisorption isotherms at 77 K and (b) pore-size distribution curve of MIL-88B(Fe)@Pt@Al-TCPP after 5 cycles.

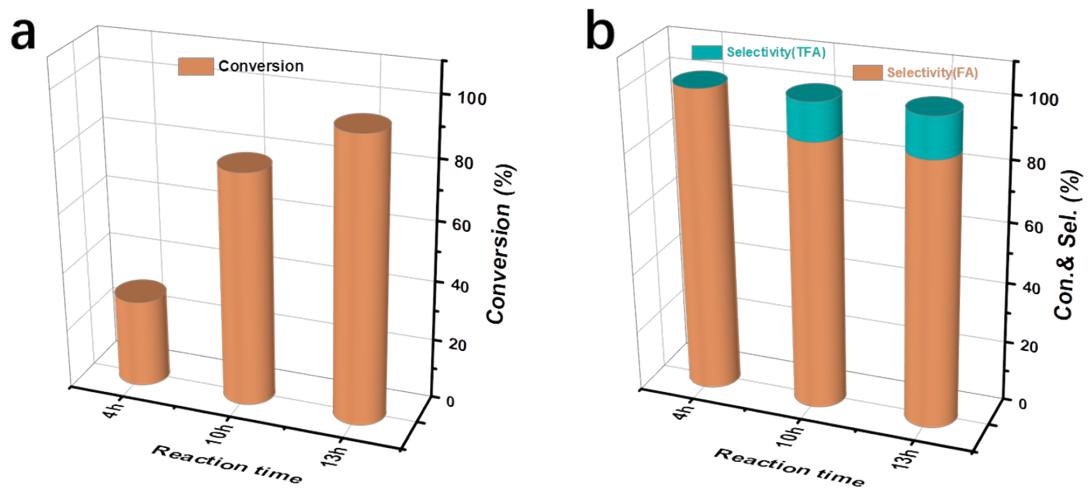


Figure S15. The conversion and selectivity data of furfural (FA) selective hydrogenation using MIL-88B(Fe)@Pt@Al-TCPP catalyst.

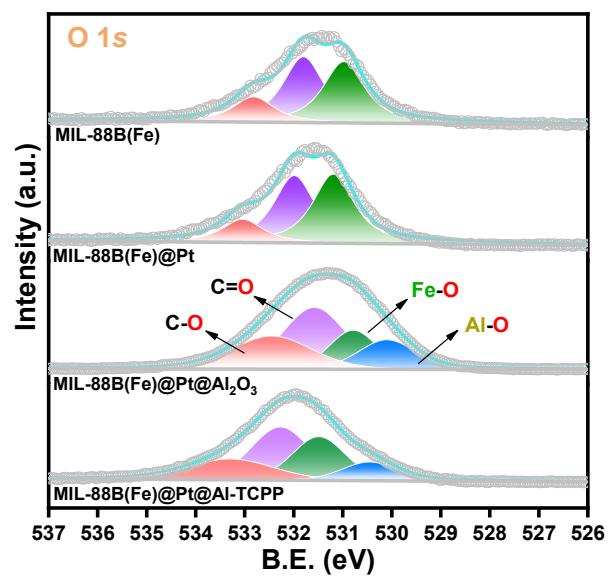


Figure S16. High-resolution O 1s spectra of MIL-88B(Fe), MIL-88B(Fe)@Pt, MIL-88B(Fe)@Pt@Al₂O₃, and MIL-88B(Fe)@Pt@Al-TCPP catalysts.

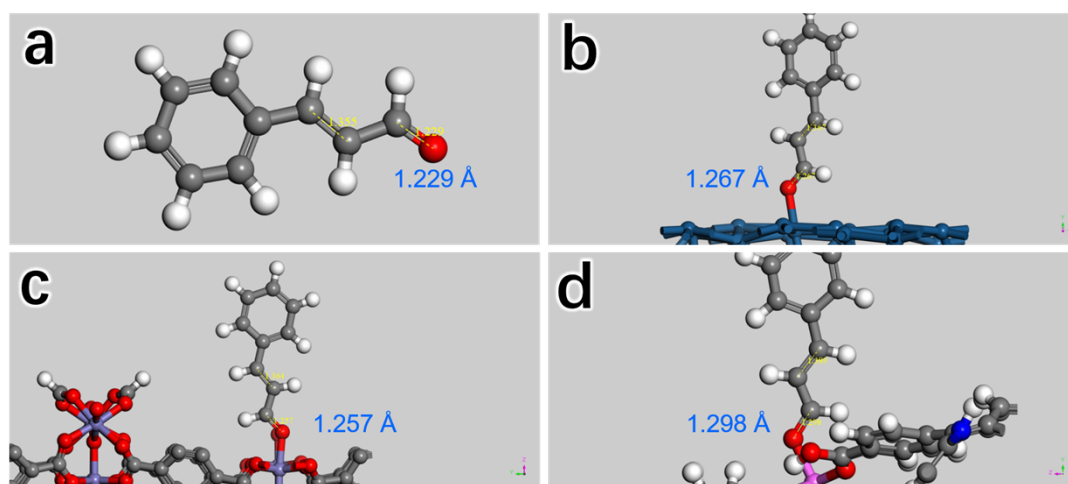


Figure S17. The bond length of the C=O double bond of (a) the free CAL molecule. The bond length of the C=O double bond of the CAL molecule adsorbed on (b) Pt NPs, (c) MIL-88B(Fe), and (d) Al-TCPP.

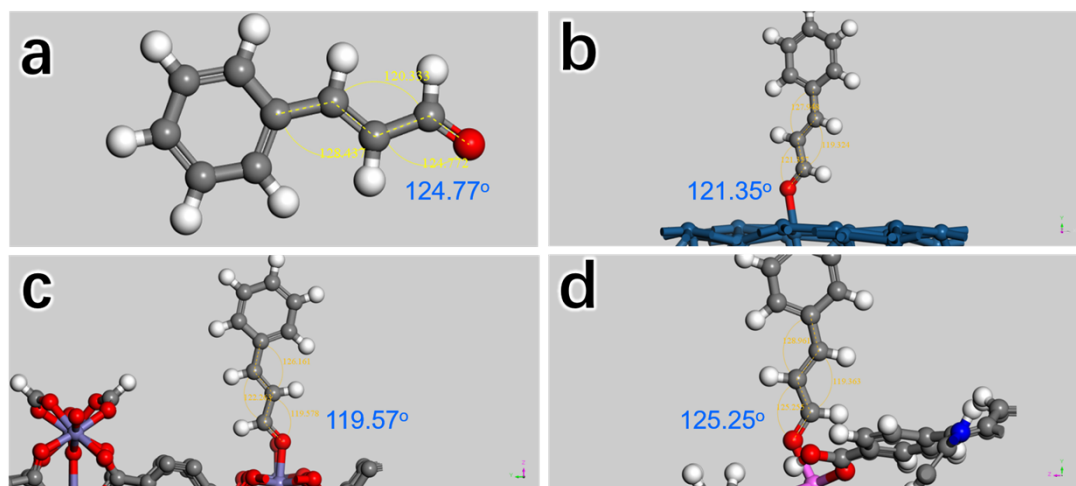


Figure S18. The bond angle of the C=O double bond of (a) the free CAL molecule. The bond angle of the C=O double bond of the CAL molecule adsorbed on (b) Pt NPs, (c) MIL-88B(Fe), and (d) Al-TCPP.

References

1. Y. C. Hong, K. Q. Sun, G. R. Zhang, R. Y. Zhong and B. Q. Xu, *Chem. Commun.*, 2011, **47**, 1300-1302.
2. K.-Q. Sun, Y.-C. Hong, G.-R. Zhang and B.-Q. Xu, *ACS Catal.*, 2011, **1**, 1336-1346.
3. H. Pan, J. Li, J. Lu, G. Wang, W. Xie, P. Wu and X. Li, *J Catal.*, 2017, **354**, 24-36.
4. Q. Wu, C. Zhang, M. Arai, B. Zhang, R. Shi, P. Wu, Z. Wang, Q. Liu, K. Liu, W. Lin, H. Cheng and F. Zhao, *ACS Catal.*, 2019, **9**, 6425-6434.
5. Y. Li, P.-F. Zhu and R.-X. Zhou, *Appl. Surf. Sci.*, 2008, **254**, 2609-2614.
6. X. Xiang, W. He, L. Xie and F. Li, *Catal. Sci. Technol.*, 2013, **3**, 2819-2827.
7. Z. Guo, C. Xiao, R. V. Maligal-Ganesh, L. Zhou, T. W. Goh, X. Li, D. Tesfagaber, A. Thiel and W. Huang, *ACS Catal.*, 2014, **4**, 1340-1348.
8. K. Yuan, T. Song, D. Wang, X. Zhang, X. Gao, Y. Zou, H. Dong, Z. Tang and W. Hu, *Angew. Chemie - Int. Ed.*, 2018, **57**, 5708-5713.
9. M. Zhao, K. Yuan, Y. Wang, G. Li, J. Guo, L. Gu, W. Hu, H. Zhao and Z. Tang, *Nature*, 2016, **539**, 76-80.
10. Y. Zhang, S. Wei, Y. Lin, G. Fan and F. Li, *ACS Omega*, 2018, **3**, 12778-12787.
11. Y. Zhang, C. Chen, W. Gong, J. Song, Y. Su, H. Zhang, G. Wang and H. Zhao, *RSC Adv.*, 2017, **7**, 21107-21113.
12. Y.-S. Shi, Z.-F. Yuan, Q. Wei, K.-Q. Sun and B.-Q. Xu, *Catal. Sci. Technol.*, 2016, **6**, 7033-7037.
13. K. B. Vu, K. V. Bukhryakov, D. H. Anjum and V. O. Rodionov, *ACS Catal.*, 2015, **5**, 2529-2533.
14. Y. Shu, T. Chen, H. C. Chan, L. Xie and Q. Gao, *Chem Asian J*, 2018, **13**, 3737-3744.